Recurrence patterns are significantly associated with the ^{18}F-FDG PET/CT radiomic features of patients with locally advanced non-small cell lung cancer treated with chemoradiotherapy

WENJU LIU[1,2], XU QIAO[3], HONG GE[4], SHENG ZHANG[5], XIAOJIANG SUN[6], JIANCHENG LI[7], WEILIN CHEN[8], WENDONG GU[9] and SHUANGHU YUAN[1,4,10]

[1]Department of Radiation Oncology, Shandong University Cancer Center, Jinan, Shandong 250117; [2]Department of Radiation Oncology, Liaocheng People's Hospital, Liaocheng, Shandong 252000; [3]School of Control Science and Engineering, Shandong University, Jinan, Shandong 250117; [4]Department of Radiation Oncology, The Affiliated Cancer Hospital of Zhengzhou University (Henan Cancer Hospital), Zhengzhou, Henan 450000; [5]Cancer Center, Union Hospital, Tongji Medical College, Huazhong University of Science and Technology, Wuhan, Hubei 430022; [6]Department of Radiation Oncology, The Cancer Hospital of the University of Chinese Academy of Sciences, Zhejiang Cancer Hospital, Hangzhou, Zhejiang 310022; [7]Department of Radiation Oncology, Fujian Cancer Hospital, College of Clinical Medicine for Oncology, Fujian Medical University, Fuzhou, Fujian 350000; [8]Department of Radiation Oncology, Zhangzhou Hospital Affiliated to Fujian Medical University, Zhangzhou, Fujian 363000; [9]Department of Radiation Oncology, The Third Hospital Afiliated to Suzhou University, Changzhou, Jiangsu 213000; [10]Department of Radiation Oncology, Shandong Cancer Hospital and Institute, Shandong First Medical University and Shandong Academy of Medical Sciences, Jinan, Shandong 250117, P.R. China

Received February 22, 2023; Accepted May 22, 2023

DOI: 10.3892/ol.2023.13903

Abstract. A model for predicting the recurrence pattern of patients with locally advanced non-small cell lung cancer (LA-NSCLC) treated with chemoradiotherapy is of great importance for precision treatment. The present study analyzed whether the comprehensive quantitative values (CVs) of the fluorine-18(^{18}F)-fluorodeoxyglucose (FDG) positron emission tomography (PET)/computed tomography (CT) radiomic features and metastasis tumor volume (MTV) combined with clinical characteristics could predict the recurrence pattern of patients with LA-NSCLC treated with chemoradiotherapy. Patients with LA-NSCLC treated with chemoradiotherapy were divided into training and validation sets. The recurrence profile of each patient, including locoregional recurrence (LR), distant metastasis (DM) and both LR/DM were recorded. In the training set of patients, the primary tumor prior radiotherapy with ^{18}F-FDG PET/CT and both primary tumors and lymph node metastasis were considered as the regions of interest (ROIs). The CVs of ROIs were calculated using principal component analysis. Additionally, MTVs were obtained from ROIs. The CVs, MTVs and the clinical characteristics of patients were subjected to aforementioned analysis. Furthermore, for the validation set of patients, the CVs and clinical characteristics of patients with LA-NSCLC were also subjected to logistic regression analysis and the area under the curve (AUC) values calculated. A total of 86 patients with LA-NSCLC were included in the analysis, including 59 and 27 patients in the training and validation sets of patients, respectively. The analysis revealed 22 and 12 cases with LR, 24 and 6 cases with DM and 13 and 9 cases with LR/DM in the training and validation sets of patients, respectively. Histological subtype, CV2-5 and CV3-4 were identified as independent variables in the logistic regression analysis ($P<0.05$). In addition, the AUC values for diagnosing LR, DM and LR/DM were 0.873, 0.711 and 0.826, and 0.675, 0.772 and 0.708 in the training and validation sets of patients, respectively. Overall, the results demonstrated that the spatial and metabolic heterogeneity quantitative values from the primary tumor combined with the histological subtype could predict the recurrence pattern of patients with LA-NSCLC treated with chemoradiotherapy.

Correspondence to: Professor Shuanghu Yuan, Department of Radiation Oncology, Shandong Cancer Hospital and Institute, Shandong First Medical University and Shandong Academy of Medical Sciences, 440 Jiyan Road, Jinan, Shandong 250117, P.R. China
E-mail: yuanshuanghu@sina.com

Key words: ^{18}F-FDG PET/CT, locally advanced non-small cell lung cancer, chemoradiotherapy, recurrence pattern

Introduction

It has been reported that the treatment of patients with locally advanced non-small cell lung cancer (LA-NSCLC) with disease recurrence after chemoradiotherapy is difficult (1-4). Precision therapy based on different recurrence patterns are a potential

strategy for reducing disease recurrence (5). Therefore, the construction of a model for predicting the recurrence pattern of patients with LA-NSCLC treated with chemoradiotherapy is of great importance for precision treatment. The recurrence patterns of patients with LA-NSCLC undergoing chemoradiotherapy can be divided into locoregional recurrence (LR), distant metastasis (DM) and both LR and DM (LR/DM) (6).

The radiomic features of fluorine-18(^{18}F)-fluorodeoxyglucose (FDG) positron emission tomography (PET)/computed tomography (CT) and the clinical characteristics of patients may potentially serve a significant role in predicting the recurrence patterns of patients with LA-NSCLC treated with chemoradiotherapy (6-9). The radiomic features of ^{18}F-FDG PET/CT, including quantitative and semi-quantitative features, commonly reflect the spatial and metabolic heterogeneity of the tumor (10). The quantitative features refer to the association between the grey level intensity of pixels or voxels and their position within an image. On the other hand, the semi-quantitative features are associated with ^{18}F-FDG uptake semi-quantitative values, such as metabolic tumor volume (MTV). A previous study showed that the primary tumor volume in patients with LA-NSCLC is significantly associated with the recurrence of the primary tumor after chemoradiotherapy (9). Therefore, tumors with a volume of >50 cm^3 are more prone to recurrence compared with those with a volume of ≤50 cm^3. Another study demonstrated that the total MTV of the primary tumor and regional metastatic lymph nodes, analyzed by pre- and mid-radiotherapy ^{18}F-FDG PET, are significantly associated with local recurrence in patients with LA-NSCLC (11). Therefore, it has been hypothesized that the deep learning model constructed based on the features of CT radiomics can be used to predict the recurrence pattern of chemoradiotherapy-treated patients with LA-NSCLC (12). It has also been suggested that the histological subtypes can be associated with the recurrence patterns of the aforementioned patients (5). A previous study demonstrated that squamous cell carcinoma is more prone to LR compared with adenocarcinoma (5). The aforementioned studies imply that the radiomic features of ^{18}F-FDG PET/CT combined with the clinical characteristics of patients can exhibit considerable accuracy in predicting the recurrence patterns of patients with LA-NSCLC undergoing chemoradiotherapy.

In the present study, patients with LA-NSCLC who received chemoradiotherapy were analyzed. In the training set of patients, to predict the recurrence pattern of patients with LA-NSCLC, logistic regression analysis was performed based on the comprehensive quantitative values (CVs) of the radiomic features of ^{18}F-FDG PET/CT, MTV and the clinical characteristics of patients. Furthermore, the logistic regression analysis results were verified in the validation set of patients.

Materials and methods

Patients. In the present study, patients with LA-NSCLC treated with chemoradiotherapy in Shandong University Cancer Center (Jinan, China), Henan Cancer Hospital (Zhengzhou, China), Union Hospital Tongji Medical College Huazhong University of Science and Technology (Wuhan, China), Zhejiang Cancer Hospital (Hangzhou, China), Fujian Cancer Hospital (Fuzhou, China), Zhangzhou Hospital Affiliated to Fujian Medical University (Zhangzhou, China) and The Third Hospital Affiliated to Suzhou University (Changzhou, China) between May 2016 and January 2020 were analyzed. The inclusion criteria were as follows: i) Non-operative patients with LA-NSCLC diagnosed by histology; ii) with Karnofsky performance status (KPS) prior to therapy of ≥70; iii) treated with concurrent or sequential chemoradiotherapy; iv) patients who underwent ^{18}F-FDG PET/CT scanning within two weeks prior radiotherapy; and v) patients whose recurrence patterns were recorded. The exclusion criteria were as follows: i) Patients with small cell lung cancer; ii) whose ^{18}F-FDG PET/CT images were missing; iii) treated with radiotherapy dose of <50 Gy (equivalent effective doses at 2 Gy per fraction); and iv) patients whose follow-up data were missing. Based on different centers where patients were treated, patients were randomly allocated into the training and validation sets of patients. The current retrospective study was approved by the Shandong University Cancer Center Medical Ethics Committee (approval no. 201511089).

^{18}F-FDG PET/CT imaging. All eligible patients underwent ^{18}F-FDG PET/CT scanning imaging (Discovery LS PET/CT system; Cytiva) within two weeks prior to radiotherapy. Before ^{18}F-FDG PET/CT scan, patients fasted and rested for at least 6 h. The blood glucose levels were <6.6 mmol/l before scanning. The patients did not receive bladder catheterization, oral muscle relaxants or CT contrast enhancers. Scanning started at 44-76 min following intravenous injection of 370 MBq (10 mCi) ^{18}F-FDG and ^{18}F-FDG PET images were obtained from the top of the skull to the proximal thigh. Each field of vision covered 14.5 cm for 5 min and the thickness of each layer was 4.25 mm in the axial direction. The peak voltage of the X-ray tube, which was used for spiral CT scan, was 120 kV and 90 mA and the thickness of each layer was 4.25 mm. ^{18}F-FDG PET/CT scan images were captured under natural breathing and were reconstructed using an ordered subset expectation maximization algorithm.

Treatment. All patients were treated with concurrent or sequential chemoradiotherapy. Intensity-modulated radiation therapy (IMRT) was used as the type of irradiation. Radiotherapy planning was performed using ^{18}F-FDG PET/CT or CT scan. No prophylactic irradiation was delivered to the lymphatic drainage area. The gross tumor volume (GTV) included the primary tumor and all metastatic lymph nodes [CT measurement short diameter of >10 mm or PET standardized uptake value (SUV) of >2.5], while the clinical target volume (CTV) included GTVs exceeding 6 mm (squamous cell carcinoma) or 8 mm (adenocarcinoma or other histological types). The planning target volume consisted of a margin extending outside the CTV, which was 5 and 10-15 mm in all directions of the ^{18}F-FDG PET and CT image, respectively. Conventional fractionated (CFRT) or late-course hyperfractionated accelerated radiotherapy (LCHART) were used for radiotherapy fractionation. CFRT was defined as a single 2-3 Gy fraction, once a day for five days/week. LCHART included two phases, CFRT and hyperfractionated accelerated radiotherapy. Hyperfractionated accelerated radiotherapy was performed following CFRT, with fractions of 1.4 Gy, twice daily. The radiotherapy dose was prescribed to the 95% isodose line of the respective

IMRT plan, covering at least 95% of the target volume. The GTV prescription dose was corrected to equivalent effective doses at 2 Gy per fraction (EQD2) using the linear quadratic model (α/β=10.0 Gy). The corrected prescription dose was used for statistical analysis. Chemotherapy regimens included platinum-based chemotherapy, two-drug combination chemotherapy or single-drug chemotherapy.

Follow-up. Follow-up was performed once every 3-6 months after treatment and included physical examination, chest CT scan and other necessary examinations, such as craniocerebral magnetic resonance examination, when headache occurred. Progression free survival (PFS) was defined as the time from ^{18}F-FDG PET/CT scan to locoregional recurrence/distant metastasis or death. Overall survival (OS) was defined as the time interval between ^{18}F-FDG PET/CT scan and patient death or last follow-up. Additionally, disease recurrence was considered as the first disease progression recorded according to the Response Evaluation Criteria in Solid Tumors (RECIST 1.1). Histological diagnosis was not necessary. Recurrence patterns included LR, DM and LR/DM. LR was characterized by the recurrence of the primary tumor and/or regional lymph nodes, while DM was defined as metastasis outside the primary tumor and regional lymph nodes. LR/DM is defined by both LR and DM.

Image analysis. For the training set of patients, the regions of interest (ROIs) were delineated using ITK-SNAP (13) or CGITA (14) software. For ITK-SNAP, the ROIs were drawn manually by a radiation oncologist with >10 years target delineation experience. For CGITA, a SUV value of 2.5 was selected to delineate ROIs using an automatic threshold-based region growing method. When the lesions were adjacent to non-lesions with high ^{18}F-FDG uptake, such as the heart and liver, the ROIs were drawn manually by the radiation oncologist. The primary tumors identified by ^{18}F-FDG PET and CT scan and drawn using ITK-SNAP software, were defined as ROI1 and ROI2, respectively. Subsequently, PyRadiomics software (15) was used to extract the quantitative values of the ROI1 and ROI2 radiomic features. In addition, the primary tumor and both the primary tumor and regional metastatic lymph nodes displayed by ^{18}F-FDG PET and delineated using CGITA software, were defined as ROI3 and ROI4, respectively. CGITA software was then used to calculate the quantitative values of the ROI3 radiomic features and extract the MTVs of ROI3 and ROI4, which were named MTV3 and MTV4. For the validation set of patients, the corresponding ROIs and quantitative values of the ROI radiomic features were also obtained as described for the training set of patients.

Statistical analysis. All statistical analyses were carried out using SPSS (V21.0; IBM Corp.) and MedCalc (V15.8; MedCalc software Ltd.). $P<0.05$ was considered to indicate a statistically significant difference. The 1- and 2-year recurrence rate of patients in the training and validation sets of patients were calculated using the following equation: Number of patients with recurrence events within 1- or 2-year/total number of patients included in the training or validation sets of patients. The logistic regression equations for predicting the recurrence patterns in the training set of patients were developed as follows: CVs were calculated using the principal component analysis according to the following formula: $CVr\text{-}i = a_{i1}X1' + a_{i2}X2' + ... + a_{im}X_m'$, where r indicates 1,2,3, i indicates 1,2,...,m, a_{im} indicates component coefficient and X_m' indicates the Z-score standardized value of ROI radiomic features quantitative values. In addition, the Z-score standardized value was calculated using the following formula: Z-score value=original value-mean value/standard deviation (SD). CVs with eigenvalues >1 were subjected to further analysis. Spearman's rank order correlation or association analysis were used to calculate the correlation and association coefficients between clinical characteristics, including CVs, MTV3, MTV4 and recurrence patterns. Unpaired two-tailed t-test or χ^2 test was applied to evaluate whether the correlation and association coefficients were statistically significant. Subsequently, the features with significant correlation or association coefficients were used to construct the logistic regression equations for predicting recurrence patterns. The probability values of recurrence patterns were measured using the logistic equations and the receiver operating characteristic (ROC) curves for diagnosing recurrence patterns were constructed based on these values. The areas under ROC curves (AUCs), cut-off, sensitivity and specificity values were calculated based on the maximum value of Youden index. The logistic regression equations for predicting the recurrence patterns were verified in the validation set of patients as follows: The corresponding CVs in the validation set of patients were obtained as described for the training set of patients. The CVs and clinical characteristics were inserted into the logistic equations. The probability values of recurrence patterns were obtained as previously described. ROC curves were constructed based on the predicted and actual recurrence patterns and the AUC, sensitivity and specificity values were then calculated.

Results

Patient characteristics and recurrence patterns. A total of 96 patients from seven centers were enrolled between May 2016 and January 2020. Among these patients, 10 patients were excluded, eight due to lack of ^{18}F-FDG PET/CT and two due to missing follow-up data. Overall, 86 patients were considered eligible for the study. The median follow-up time was 21.5 months (range, 2.8-61.8 months), while the median PFS and OS were 9.3 [95% confidence interval (CI), 7.7-11.0 months] and 32.0 months (95% CI, 17.6-46.4 months), respectively. A total of 59 patients from five centers were included in the training set of patients and 27 patients from two centers in the validation set of patients. The flow diagram illustrating the study enrollment process is shown in Fig. 1. The clinical characteristics of patients are listed in Table I. For the training set of patients, the median age was 60 years (range, 39-73 years), the radiotherapy dose was 60.00 Gy (range, 60.00-75.91 Gy), while chemotherapy lasted for four cycles (range, 1-7 cycles). In addition, the median follow-up time was 23.5 months (range, 3.9-41.8 months), while the median PFS and OS were 9.4 (95% CI, 7.6-11.2 months) and 31.0 months (95% CI, 20.8-41.2 months), respectively. A total of 22 patients experienced LR, accounting for 37.3% of all cases, while 24 patients experienced DM (40.7%) and 13 patients experienced LR/DM (22.0%). The 1- and 2-year recurrence rates were 67.8 and 88.1%, respectively. For the validation set of patients, the median age was

Table I. Patient characteristics in the training and validation sets of patients.

	Training set		Validation set	
Characteristic	Number	%	Number	%
Age (years)				
≤60	33	55.9	13	48.1
>60	26	44.1	14	51.9
Sex				
Male	50	84.7	22	81.5
Female	9	15.3	5	18.5
Histology				
SCC	41	69.5	17	63.0
ADC	18	30.5	8	29.6
Other	0	0	2	7.4
Stage[a]				
IIIA	15	25.4	12	44.4
IIIB	32	54.2	9	33.3
IIIC	12	20.3	6	22.2
Karnofsky performance status scoe				
70	3	5.1	1	3.7
80	18	30.5	8	29.6
90	36	61.0	16	59.3
100	2	3.4	2	7.4
Smoking index				
0	14	23.7	10	37.0
1-400	8	13.6	4	14.8
>400	37	62.7	12	44.4
Treatment model				
CCRT	53	89.8	17	63.0
SCRT	6	10.2	10	37.0
Radiotherapy dose[b] (Gy, GTV)				
≤60	34	57.6	12	44.4
>60	25	42.4	15	55.6
Chemotherapy cycles (n)				
1-4	47	79.7	22	81.5
>4	12	20.3	5	18.5

[a]International Association for the Study of Lung Cancer (IASLC) staging, 8th edition; [b]equivalent effective doses at 2 Gy per fraction. GTV, gross tumor volume; SCC, squamous cell carcinoma; ADC, adenocarcinoma; CCRT, concurrent chemoradiotherapy; SCRT, sequential chemoradiotherapy.

58 years (range, 34-86 years), the median radiotherapy dose was also 60.00 Gy (range, 50.00-75.25 Gy) and chemotherapy also lasted for four cycles (range, 1-6 cycles). Additionally, the median follow-up period was 18.9 months (range, 2.8-61.8 months), while the median PFS and OS were 9.3 (95% CI, 4.2-14.5 months) and 40.4 months (95% CI, 30.4-50.4 months), respectively. There were 12 patients with LR (44.4%), six patients with DM (22.2%) and nine patients with LR/DM (33.3%). Finally, the 1- and 2-year recurrence rates were 63.0 and 88.9%, respectively.

CVs and MTVs in the training set of patients. Retrospective ROI examples are shown in Fig. 2. A total of 86, 100 and 72 quantitative values of radiomic features were extracted from ROI1, ROI2 and ROI3, respectively (Table SI). The mean ± SD values are listed in Table SI. The CVs included 86 CV1 (CV1-1-CV1-86), 100 CV2 (CV2-1-CV2-100) and 72 CV3 (CV3-1-CV3-72). The mean ± SD values of MTV3 and MTV4 were 88.97±114.79 and 118.39±136.91 cm^3, respectively. Among these CVs, nine CV1, 10 CV2 and nine CV3 were selected for further analysis. These CVs and their eigenvalues are shown in Table SII.

Recurrence pattern prediction in the training set of patients. Analysis revealed that histological subtypes CV2-5, CV2-7 and

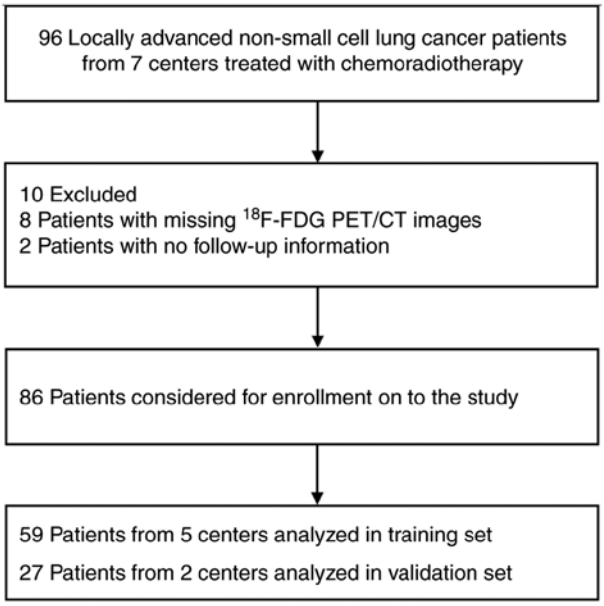

Figure 1. Flow diagram of study enrollment. ^{18}F-FDG PET/CT, fluorine-18-fluorodeoxyglucose positron emission tomography/computed tomography.

Table II. Correlation and association coefficients between histology type, CVs and recurrence patterns in the training set of patients.

	Recurrence patterns[a]	
Feature	Correlation coefficient	P-value
Histology type[b]	0.449[c]	0.001
CV2-5	0.259[d]	0.048
CV2-7	-0.282[d]	0.031
CV3-4	-0.365[d]	0.004

[a]Locoregional recurrence, distant metastasis, both of locoregional recurrence and distant metastasis; [b]squamous cell carcinoma and adenocarcinoma; [c]association coefficient; [d]Spearman correlation coefficient. CV, comprehensive quantitative value; CV2-5, the fifth CV of ROI2 radiomics features; CV2-7, the seventh CV of ROI2 radiomics features; CV3-4, the fourth CV of ROI3 radiomics features; ROI2, the primary tumor ROI displayed by CT using ITK-SNAP delineation; ROI3, the primary tumor ROI displayed by ^{18}F-FDG PET using CIGITA delineation.

CV3-4 were significantly associated with recurrence patterns (Table II). No significant association was obtained between age, sex, clinical stage, KPS, smoking index, treatment model, radiotherapy dose, chemotherapy cycle, MTV3, MTV4 and the other 25 CVs and recurrence patterns (data not shown). The logistic regression equations for predicting recurrence patterns are listed in Table III. The logistic equations identified histological subtype and two CVs, namely CV2-5 and CV3-4, as significant independent variables. The ROC curves used for diagnosing recurrence patterns are presented in Fig. 3A-C. For diagnosing LR, the AUC, cut-off, sensitivity and specificity values were 0.873, 0.560, 0.682 and 0.946, respectively. In addition, the AUC, cut-off, sensitivity and specificity values for diagnosing DM were 0.826, 0.370, 0.750 and 0.829, respectively, while the corresponding values for diagnosing LR/DM were 0.772, 0.170, 0.846 and 0.609, respectively.

Efficiency of the prediction model in the validation set. A total of 27 patients were allocated to the validation set of patients, including 25 patients with squamous cell carcinoma/adenocarcinoma and two patients with other histological subtypes. However, the recurrence pattern prediction model constructed in the training set of patients included only patients with squamous cell carcinoma/adenocarcinoma. Therefore, 25 patients with squamous cell carcinoma/adenocarcinoma were used to verify the recurrence pattern prediction model, while the two patients with the other histological subtypes were excluded. Representative examples for ROI2 and ROI3 are shown in Fig. 2. The corresponding mean ± SD values are listed in Table SIII, while the values of CV2-5 and CV3-4 are shown in Table SIV. Furthermore, the ROC curves for diagnosing recurrence patterns are presented in Fig. 4A-C. Therefore, the AUC, sensitivity and specificity values for diagnosing LR were 0.711, 0.636 and 0.786, respectively. The AUC, sensitivity and specificity values for diagnosing DM and LR/DM were 0.675, 0.600 and 0.750 and 0.708, 0.667 and 0.750, respectively.

Discussion

It has been previously reported that the prognosis of patients with LA-NSCLC treated with chemoradiotherapy is poor, as the majority of these patients may experience disease recurrence after chemoradiotherapy (8,16-18). The present study showed that the 1 year recurrence rate was 67.8 and 63.0% in the training and validation sets of patients, respectively. A randomized controlled study (RTOG0617) demonstrated that the 1 year recurrence rate of patients with LA-NSCLC treated with 60 Gy conventional radiotherapy combined with chemotherapy is 49.2% (16). Additionally, a previous retrospective study demonstrated that the total recurrence rate for patients with LA-NSCLC who underwent chemoradiotherapy is 65.9% (17). Furthermore, another retrospective study showed that the 1 year recurrence rate of LA-NSCLC is 74% (19). The aforementioned results indicate that the majority of patients with LA-NSCLC can experience disease recurrence after chemoradiotherapy. Therefore, precision treatment should be considered to reduce disease recurrence.

The current study also demonstrated that CV2-5 and CV3-4 combined with histological subtype could predict the recurrence patterns of chemoradiotherapy-treated patients with LA-NSCLC. CV2-5 and CV3-4 were the linear combination and were composed of the radiomic feature quantitative values from the primary tumors imaged using ^{18}F-FDG PET/CT. Therefore, CV2-5 and CV3-4 could reflect the spatial and metabolic heterogeneity of the primary tumors. The higher the CV2-5 value, the higher the probability for LR/DM. However, a lower CV2-5 value was associated with a higher probability for LR. Additionally, a greater CV3-4 value was associated with an increased risk for LR, while the lower value was associated with a greater probability for DM and LR/DM. The results also demonstrated that patients with squamous cell carcinoma were prone to LR, while those with adenocarcinoma were prone to DM. The aforementioned

Table III. Logistic regression equations for predicting recurrence patterns in the training set of patients[a].

Predicted recurrence pattern	Feature	Coefficient	P-value	Hazard ratio	95% Confidence interval	
					Lower	Upper
DM	Histology type[b]	-2.768	0.006	0.063	0.009	0.447
	CV3-4	-1.280	0.008	0.278	0.108	0.716
	Constant	2.353	0.012	-	-	-
LR/DM	CV2-5	0.933	0.041	2.542	1.037	6.232
	CV3-4	-1.580	0.003	0.206	0.072	0.591

[a]Locoregional recurrence as reference; [b]squamous cell carcinoma is 1 and adenocarcinoma is 0. DM, distant metastasis; CV, comprehensive quantitative value; LR/DM, locoregional recurrence and distant metastasis; CV2-5, the fifth CV of ROI2 radiomics features; CV3-4, the fourth CV of ROI3 radiomics features; ROI2, the primary tumor ROI displayed by CT using ITK-SNAP delineation; ROI3, the primary tumor ROI displayed by ^{18}F-FDG PET using CIGITA delineation; CV2-5, the fifth CV of ROI2 radiomics features; CV3-4, the fourth CV of ROI3 radiomics features.

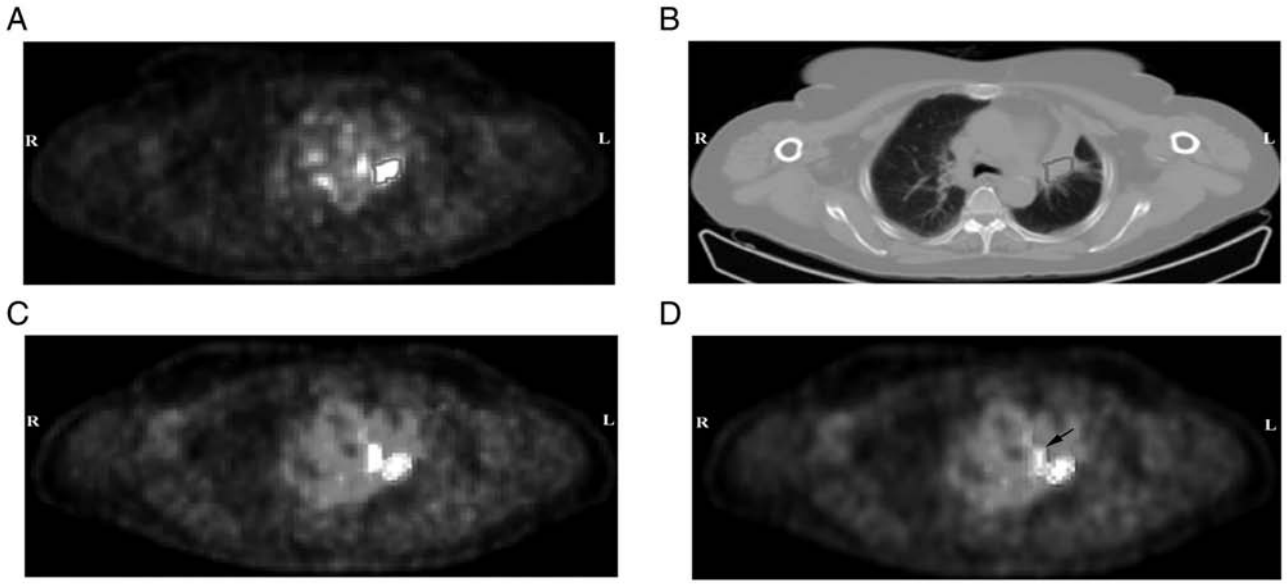

Figure 2. ROIs obtained by ^{18}F-FDG PET/CT scan. Primary tumor ROIs obtained by (A) ^{18}F-FDG PET(ROI1) and (B) CT (ROI2) scan were created using ITK-SNAP software. (C) Primary tumor (ROI3) and (D) both primary tumor and metastatic lymph node (ROI4) ROIs that resulted from ^{18}F-FDG PET were drawn using CIGITA software. (D) Metastatic lymph node ROI was indicated by the black arrow. ROI, region of interest; ^{18}F-FDG PET/CT, fluorine-18-fluorodeoxyglucose positron emission tomography/computed tomography.

findings indicated that the recurrence patterns were different for patients with LA-NSCLC treated with chemoradiotherapy and were associated with CV2-5, CV3-4 and histological subtype. Therefore, to reduce the disease recurrence rate, different treatment approaches should be considered according to different CV2-5, CV3-4 and histological subtypes.

Furthermore, the present study demonstrated that the CV2-5 of the pre-radiotherapy CT scan radiomic features was also markedly associated with the recurrence patterns of chemoradiotherapy-treated patients with LA-NSCLC. In addition, CV2-5 combined with CV3-4 and histological subtype could also predict the recurrence patterns of the aforementioned patients. A previous retrospective study reported that the deep learning model constructed by radiomic features of pre- and post-treatment CT scans can also predict the recurrence patterns of patients with LA-NSCLC (12). Consistent with the results of the current study, previous research also indicated that patients with squamous cell carcinoma are more prone to LR compared with those suffering from adenocarcinoma (5). These findings suggest that enhancing local and systemic treatment to reduce LR and DM in patients with squamous cell carcinoma and adenocarcinoma could be the appropriate approach for patients with LA-NSCLC undergoing chemoradiotherapy.

Previous studies showed that the MTVs of the primary tumor and regional metastatic lymph nodes displayed by ^{18}F-FDG PET pre- and mid-radiotherapy are significantly associated with the recurrence patterns of patients with LA-NSCLC who receive chemoradiotherapy (11). The AUC values of pre- and mid-radiotherapy MTVs for predicting LR are 0.71 and 0.76,

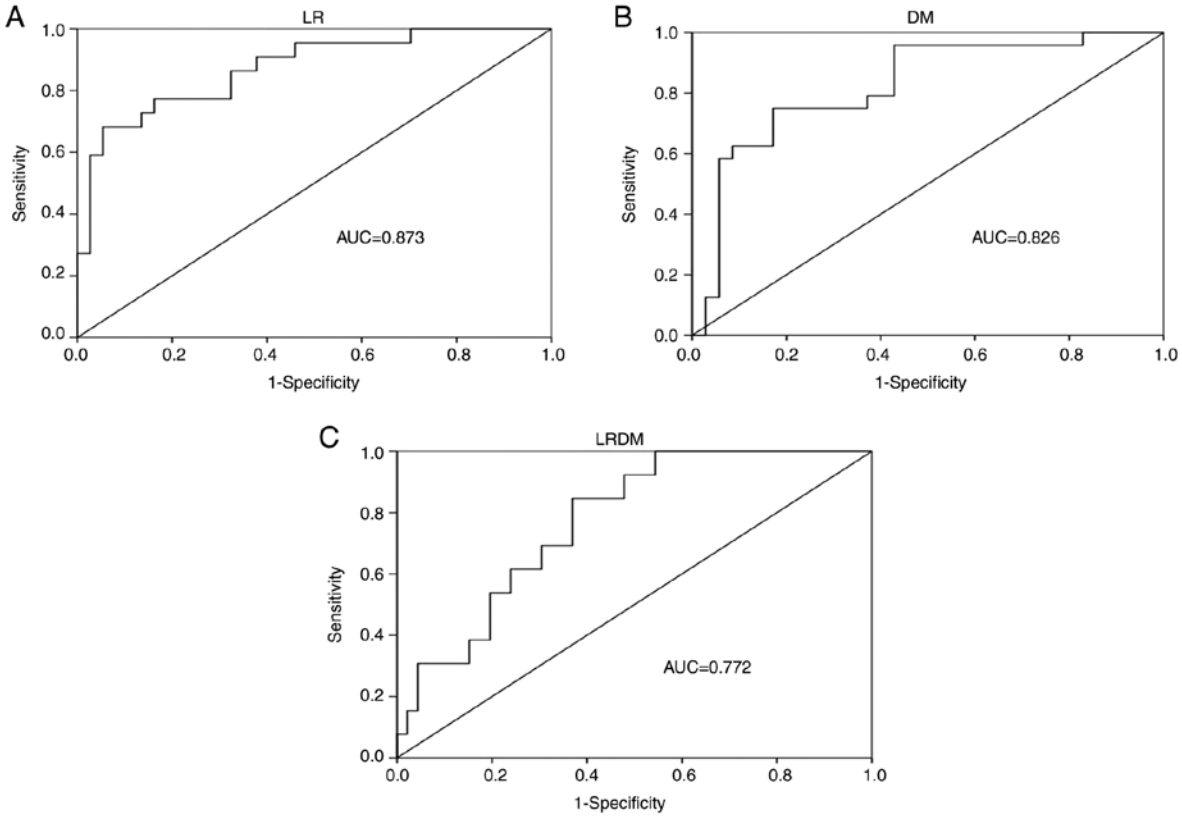

Figure 3. ROC curves for identifying recurrence patterns in the training set of patients. ROC curves for diagnosing (A) LR, (B) DM and (C) LR/DM. LR, locoregional recurrence; DM, distant metastasis; ROC, receiver operating characteristic; AUC, area under the curve.

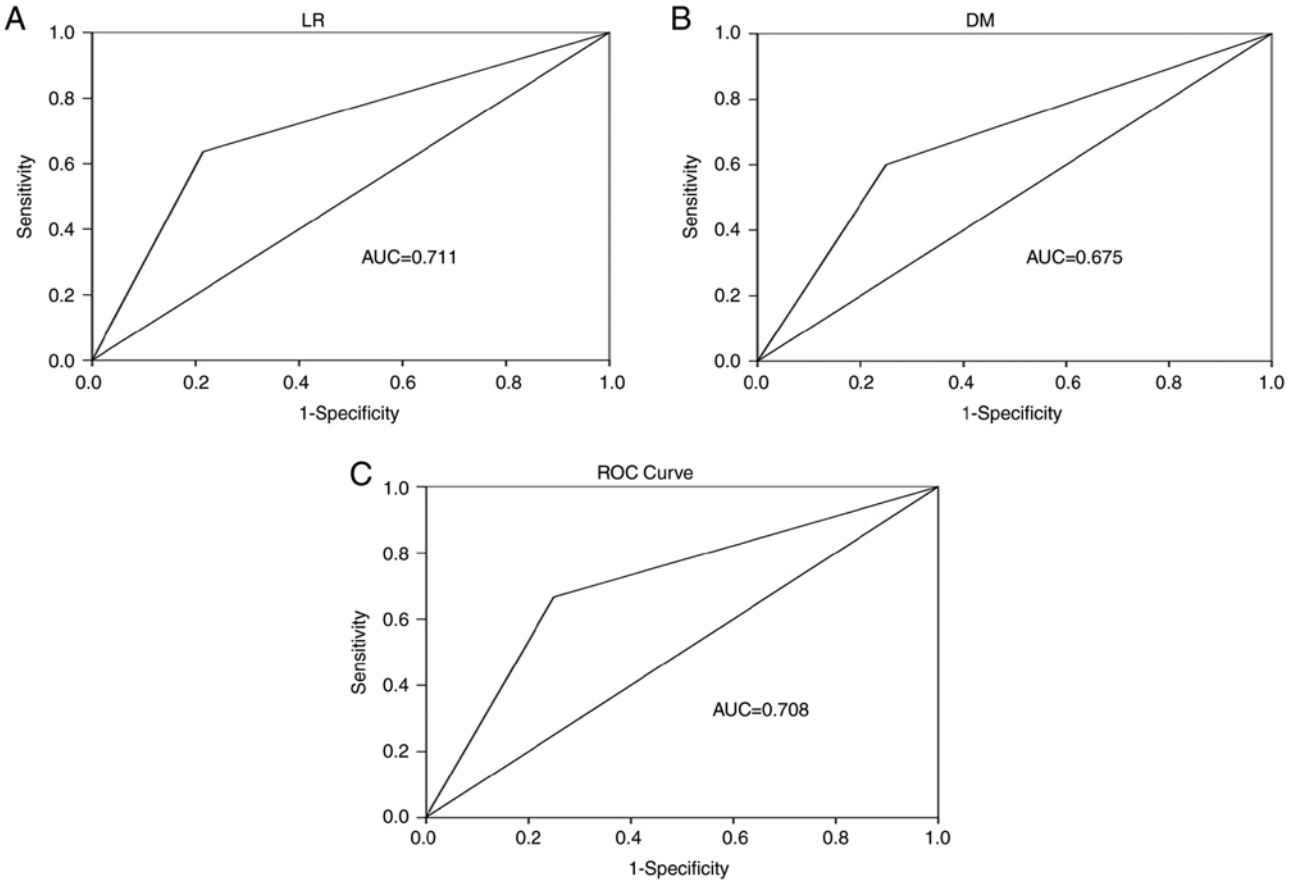

Figure 4. ROC curves for diagnosing recurrence patterns in the validation set of patients. ROC curves for diagnosing (A) LR, (B) DM and (C) LR/DM. LR, locoregional recurrence; DM, distant metastasis; ROC, receiver operating characteristic; AUC, area under the curve.

respectively (11). A previous study demonstrated that patients with LA-NSCLC and a tumor volume >50 cm^3 are more prone to primary tumor recurrence after chemoradiotherapy compared with those with a tumor volume ≤50 cm^3 (9). These two retrospective studies suggested that tumor volume could be significantly associated with local recurrence in patients with LA-NSCLC treated with chemoradiotherapy. In addition, the results of the present study demonstrated that neither the MTV of the primary tumor (MTV3) nor the MTV of the primary tumor combined with regional metastatic lymph nodes (MTV4) were notably associated with the recurrence patterns of chemoradiotherapy-treated patients with LA-NSCLC. However, further studies are needed to verify whether MTVs in mid-radiotherapy could be significantly associated with the recurrence patterns of these patients.

The present retrospective study has some limitations, including the loss of particular clinical follow-up data and patient selective bias. Therefore, further research with a larger sample size of patients is needed to verify the results of the current study.

In conclusion, the present study showed that spatial and metabolic heterogeneity quantitative values from the primary tumor combined with histological subtype could predict the recurrence patterns of patients with LA-NSCLC treated with chemoradiotherapy.

Acknowledgements

Not applicable.

Funding

This study was partially funded by the Natural Science Foundation of China (grant nos. NSFC81872475 and NS FC82073345) and the Jinan Clinical Medicine Science and Technology Innovation Plan (grant no. 202019060).

Availability of data and materials

The datasets used and/or analyzed during the current study are available from the corresponding author on reasonable request.

Authors' contributions

SY conceived and designed the experiments and supervised the project. WL, XQ, HG, SZ, XS, JL, WC and WG performed the experiments. WL and XQ analyzed the data. WL wrote the manuscript. All authors read and approved the final version of the manuscript. SY and WL confirm the authenticity of all the raw data.

Ethics approval and consent to participate

This retrospective study was approved by the Shandong University Cancer Center Medical Ethics Committee (approval no. 201511089). Due to the retrospective nature of the study, the Medical Ethics Committee waived the requirement for obtaining informed consent.

Patient consent for publication

Not applicable.

Competing interests

The authors declare that they have no competing interests.

References

1. Gelb AF, Tashkin DP, Epstein JD, Szeftel A and Fairshter R: Physiologic characteristics of malignant unilateral main-stem bronchial obstruction. Diagnosis and Nd-YAG laser treatment. Am Rev Respir Dis 138: 1382-1385, 1988.
2. Kim EY, Chapman TR, Ryu S, Chang EL, Galanopoulos N, Jones J, Kubicky CD, Lee CP, The BS, Traughber BJ, *et al*: ACR Appropriateness Criteria® nonspine bone metastases. J Palliat Med 18: 11-17, 2015.
3. Chow E, Harris K, Fan G, Tsao M and Sze WM: Palliative radiotherapy trials for bone metastases: A systematic review. J Clin Oncol 25: 1423-1436, 2007.
4. Howell DD, James JL, Hartsell WF, Suntharalingam M, Machtay M, Suh JH, Demas WF, Sandler HM, Kachnic LA and Berk LB: Single-fraction radiotherapy versus multifraction radiotherapy for palliation of painful vertebral bone metastasesequivalent efficacy, less toxicity, more convenient: A subset analysis of Radiation Therapy Oncology Group trial 97-14. Cancer 119: 888-896, 2013.
5. Ito H, Matsuo Y, Ohtsu S, Nishimura T, Terada Y, Sakamoto T and Mizowaki T: Impact of histology on patterns of failure and clinical outcomes in patients treated with definitive chemoradiotherapy for locally advanced non-small cell lung cancer. Int J Clin Oncol 25: 274-281, 2020.
6. Lou F, Sima CS, Rusch VW, Jones DR and Huang J: Differences in patterns of recurrence in early stage versus locally advanced non-small cell lung cancer. Ann Thorac Surg 98: 1755-1760; discussion 1760-1, 2004.
7. Lacoppidan T, Vogelius IR, Pøhl M, Strange M, Persson GF and Nygård L: An investigative expansion of a competing risk model for first failure site in locally advanced non-small cell lung cancer. Acta Oncol 58: 1386-1392, 2019.
8. Jouglar E, Isnardi V, Goulon D, Ségura-Ferlay C, Ayadi M, Dupuy C, Douillard JY, Mahé MA and Claude L: Patterns of locoregional failure in locally advanced non-small cell lung cancer treated with definitive conformal radiotherapy: Results from the Gating 2006 trial. Radiother Oncol 126: 291-299, 2018.
9. Abe T, Kobayashi N, Aoshika T, Ryuno Y, Saito S, Igari M, Hirai R, Kumazaki YU, Miura YU, Kaira K, *et al*: Pattern of local failure and its risk factors of locally advanced non-small cell lung cancer treated with concurrent chemo-radiotherapy. Anticancer Res 40: 3513-3517, 2020.
10. Chicklore S, Goh V, Siddique M, Roy A, Marsden PK and Cook GJ: Quantifying tumour heterogeneity in 18F-FDG PET/CT imaging by texture analysis. Eur J Nucl Med Mol Imaging 40: 133-140, 2013.
11. Binkley MS, Koenig JL, Kashyap M, Xiang M, Liu Y, Sodji Q, Maxim PG, Diehn M, Loo BW Jr and Gensheimer MF: Predicting per-lesion local recurrence in locally advanced non-small cell lung cancer following definitive radiation therapy using pre- and mid-treatment metabolic tumor volume. Radiat Oncol 15: 114, 2020.
12. Xu Y, Hosny A, Zeleznik R, Parmar C, Coroller T, Franco I, Mak RH and Aerts HJWL: Deep learning predicts lung cancer treatment response from serial medical imaging. Clin Cancer Res 25: 3266-3275, 2019.
13. Yushkevich PA, Piven J, Hazlett HC, Smith RG, Ho S, Gee JC and Gerig G: User-guided 3D active contour segmentation of anatomical structures: Significantly improved efficiency and reliability. Neuroimage 31: 1116-1128, 2006.
14. Fang YH, Lin CY, Shih MJ, Wang HM, Ho TY, Liao CT and Yen TC: Development and evaluation of an opensource software package 'CGITA' for quantifying tumor heterogeneity with molecular images. Biomed Res Int 2014: 248505, 2014.
15. van Griethuysen JJM, Fedorov A, Parmar C, Hosny A, Aucoin N, Narayan V, Beets-Tan RGH, Fillion-Robin JC, Pieper S and Aerts HJWL: Computational radiomics system to decode the radiographic phenotype. Cancer Res 77: e104-e107, 2017.
16. Bradley JD, Paulus R, Komaki R, Masters G, Blumenschein G, Schild S, Bogart J, Hu C, Forster K, Magliocco A, *et al*: Standard-dose versus high-dose conformal radiotherapy with concurrent and consolidation carboplatin plus paclitaxel with or without cetuximab for patients with stage IIIA or IIIB nonsmall-cell lung cancer (RTOG 0617): A randomised, two-by-two factorial phase 3 study. Lancet Oncol 16: 187-199, 2015.

17. Kaderbhaï CG, Coudert B, Bertaut A, Adnet J, Favier L, Lagrange A, Peignaux-Casasnovas K, Mettey L, Tharin Z, Foucher P and Martin E: Outcomes of concurrent radiotherapy with weekly docetaxel and platinum-based chemotherapy in stage III non-small-cell lung cancer. Cancer Radiother 24: 279-287, 2020.
18. Spina R, Chu SY, Chatfield M, Chen J, Tin MM and Boyer M: Outcomes of chemoradiation for patients with locally advanced non-small-cell lung cancer. Intern Med J 43: 790-797, 2013.
19. Grass GD, Naghavi AO, Abuodeh YA, Perez BA and Dilling TJ: Analysis of relapse patterns after definitive chemoradiotherapy in locally advanced non-small-cell lung cancer patients. Clin Lung Cancer 20: e1-e7, 2019.